Poly(phenyl sulfone) hollow fiber forward osmosis membrane for saline water desalination

Article *in* Chemical Engineering and Processing - Process Intensification · September 2020

DOI: 10.1016/j.cep.2020.108119

3 authors:

Mariam J. Jaafer
University of Misan
1 PUBLICATION **23** CITATIONS
SEE PROFILE

Jenan Al-Najar
University of Technology, Iraq
13 PUBLICATIONS **144** CITATIONS
SEE PROFILE

Qusay Alsalhy
University of Technology-Iraq
189 PUBLICATIONS **3,236** CITATIONS
SEE PROFILE

Chemical Engineering & Processing: Process Intensification 157 (2020) 108119

Contents lists available at ScienceDirect

Chemical Engineering and Processing - Process Intensification

journal homepage: www.elsevier.com/locate/cep

Poly(phenyl sulfone) hollow fiber forward osmosis membrane for saline water desalination

Mariam J. Jaafer, Jenan A. Al-Najar, Qusay F. Alsalhy *

Membrane Technology Research Unit, Chemical Engineering Department, University of Technology, Alsinaa Street 52, Baghdad, Iraq

ARTICLE INFO

Keywords:
Nanofiltration membrane
Hollow fibers
Forward osmosis
PPSU
Water desalination
Draw solution

ABSTRACT

Different PPSU nanofiltration (NF) fibers were used for the first time as a potential fiber for saline water desalination by forward osmosis (FO). The characteristics of fibers, such as their surface structure, cross-sectional structure, and thickness were measured using a SEM and an AFM, with fiber porosity also measured. The effects of the PPSU amount and operating conditions on the performance of water transport were investigated. The structural parameter (S = 467–601) displayed small values for three PPSU fibers due to their high porosity and because the fiber was less thick, which corresponded well to their performance. The prepared PPSU fiber tested under the FO process displayed high water fluxes utilizing 3.0 M NaCl as the draw solution. High salt rejection for all PPSU FO fibers was obtained, and the salt reverse fluxes were preserved below 7.30, 6.58, and 3.89 gMH for PPSU 25, 29, and 30 wt.%, respectively. Increasing the PPSU amounts led to decreasing the specific reverse salt flux. The PPSU NF hollow fibers prepared in this work are eligible FO membranes for water desalination.

1. Introduction

Water is one of the essential compounds for humans and other organisms. With increasing population growth and the demand for water for various needs, such as drinking as well as industrial uses, the shortage of water has become a persistent global problem. There are several methods to tackle the water scarcity problem. One of these reliable methods is the desalination of seawater and saltwater in general. Desalination is a separation process that detaches salt from water to obtain fresh water [1,2]. This technology has become an important fresh water source [3,4]. Water containing less than 1000 mg L^{-1} salts or total dissolved solids (TDS) can be called fresh water [5]. Many technologies for desalination processes have been developed, with more under research and development. Generally, desalination technologies can be classified as thermal or membrane technologies. These technologies require high amounts of energy to operate the process and produce fresh water [3]. However, membrane separation technology consumes less energy compared to thermal processes, making it more favorable for desalination [6,7].

The use of membranes in the process of purification has become very common, not only for water desalination but also to remove a wide range of impurities [8]. The most common membrane processes are reverse osmosis (RO), nanofiltration (NF), ultrafiltration (UF), and microfiltration (MF). Among them, RO has been the most widely used for several decades. The RO desalination process uses hydraulic pressure high enough to overcome the osmotic pressure of saline water, and therefore, requires high energy compared to the other membrane separation processes [9]. Energy significantly influences the cost of desalination. Hence, reducing the energy demand renders the desalination process more feasible.

In recent years, the forward osmosis process has become an emerging technology for the desalination of saline water, which has several advantages compared to the reverse osmosis process and other desalination technologies: low energy, high rejection of a wide range of contaminants, and low membrane fouling [10]. The FO process depends on the chemical potential between two solutions that have different concentrations separated by a semipermeable membrane. Due to the osmotic pressure difference, water transport results from using a feed solution (FS) with a low concentration and an osmotic pressure of π_F along with a draw solution (DS) with a higher concentration and an osmotic pressure of π_D [11]. Based on the second law of thermodynamics, the driving force for the FO process is the water chemical potential (μ_{w+}) difference between the DS (low $\mu_{w,D}$) and the FS (high $\mu_{w,F}$) (see Eq. 1) [10,12].

$$\Delta\mu_w = \mu_{W,F} - \mu_{W,D} \quad (1)$$

Forward osmosis has proven to be an efficient process in various

* Corresponding author.
E-mail address: 80006@uotechnology.edu.iq (Q.F. Alsalhy).

https://doi.org/10.1016/j.cep.2020.108119
Received 27 February 2020; Received in revised form 19 August 2020; Accepted 28 August 2020
Available online 1 September 2020

Nomenclature

A	Water Permeability Coefficient (l/m^2.h.bar)
A_m	Area of membrane (m^2)
B	Salt permeability coefficient (m/s)
CF	Feed side concentration (gm/L)
CP	Permeate side concentration (gm/L)
D	Solute diffusion coefficient (m^2/s)
D*	Mean pore size (nm)
d_{in}	Inner diameter (cm)
d_{out}	Outer diameter (cm)
G	Measured weight (gm)
ID	Inner diameter (μm)
J_S	Salt flux (LMH)
J_W	Water flux (l/m^2 hr)
M	Solution molarity (mol/L)
P	Pressure (bar)
QDS	Draw solution flow rate (L/min)
QFS	Feed solution flow rate (L/min)
Ra	Mean roughness (nm)
R_g	General gas constant (L atm/mol K)
R_{rms}	The root mean square (nm)
Rs	Rejection Percentage
RSF	Reverse salt flux (g/m^2 hr)
S	Structural parameter (μm)
SRSF	Specific reverse salt flux (gm/L)
T	Temperature (K)
t	Membrane thickness (m)

applications, in addition to water desalination, such as water treatment, sewer mining, wastewater reclamation, RO brine treatment, dye wastewater treatment, and the concentration of protein solutions [13–15]. Despite the good performance of the FO process, there are a few obstacles that must be overcome for a perfectly integrated process, such as fouling and internal concentration polarization (ICP), which can be managed by identifying suitable membranes and draw solutions that are highly efficient and easily retrieved [16,17].

Similar to the RO process, the forward osmosis process uses semi-permeable membranes that must (1) have a high ability to separate water from dissolved solids, (2) provide high permeability of water, (3) provide high salt rejection, (4) considerably reduce the internal and external concentration polarization (ICP and ECP), (5) provide mechanical resistance, and (6) provide chemical stability. Moreover, a good DS should have specific properties, such as a higher water flux, lower reverse solute flux (RSF), zero toxicity, moderately low cost, and easy reclamation [12,18].

Many polymers were selected and tested in the manufacture of membranes (i.e., thin film composite membrane [TFC]) that have a hydrophilic property to use in the forward osmosis process, such as polysulfone (PSF), polybenzimidazole (PBI), polyamide (PA), polyvinylpyrrolidone (PVP), polyvinylidene fluoride (PVDF), polyacrylonitrile (PAN), polysulfone (PSU), poly (phenyl sulfone) (PPSU), and polyethersulfone (PESU) [19–21]. One of these polymers, PPSU, has beneficial properties, such as good resistance to chemical compounds, good hydrolysis stability, mechanical strength, and a good glass transition temperature [21]. The remarkable physical and chemical properties with relatively low price of PPSU resin make it prominent candidate for the fabrication of the next generation of NF hollow fibers for FO applications.

The cost for fabricating FO membrane is also a big issue that has yet to be overcome. Up to date, most available membranes used in the FO are composite membranes. Typically, the preparation of FO membranes is conducted by preparation of a highly porous support layer and formation of a selective layer producing thin-film composite membrane (TFC). The selective layer is usually prepared via interfacial polymerization reaction between two highly reactive monomers. Almost all TFC membranes are exclusively produced by the reaction of m-phenylene diamine (MPD) in the aqueous phase with 1, 3, 5-benzenetricarbonyl chloride (TMC) in the organic phase [16,18]. However, this method of preparing FO membranes includes extra cost due to the use of special materials. Therefore, in this approach, it was synthesized the FO membrane in hollow fiber configuration in a single step which makes this membrane more favorable in terms of cost and ease of preparation.

In 2007, Wang et al. [22] explored the use of a PBI NF membrane as an FO membrane. PBI was chosen due to its unique NF characteristics. Good salt rejection and high water flux were obtained utilizing the PBI NF membrane. They concluded that the PBI NF membrane was a promising membrane with a desirable mean pore size for the FO process [22]. Accordingly, based on what was found from the positive results of using the PBI NF membrane in FO process [22], potential PPSU NF hollow fibers were prepared at various PPSU concentrations for the desalination of saline water by FO hollow fiber, which is explored for the first time in this work. PPSU hollow fibers were characterized to investigate the morphological structure, porosity, and thickness of the prepared fibers for the FO membrane. The operating conditions of the FO process, such as the concentration and flowrate of both the feed and draw solutions on the water flux, was also studied.

2. Materials and methods

2.1. Materials

PPSU (Radel R-5000, with an average Mw = 50 KDa and specific gravity = 1.28) was provided by Solvay Advanced Polymers (Belgium). N-methyl-2-pyrrolidone (NMP) (99.5 %) was used as the polymer solvent, purchased from Sigma-Aldrich (St. Louis, MO). Sodium chloride (NaCl) (Sigma-Aldrich, Assay 99.5 % min) was also used.

2.2. Membrane fabrication

In the fabrication of NF hollow fibers it is obvious that the polymer concentration should be in the range of higher than 23 wt.% in the dope solution [21,22]. Also, to make sure that the selective layer of the NF hollow fiber is formed at the outer surface (shell side), therefore, this study employed a poly(phenyl sulfone) (PPSU) hollow fiber membrane prepared from different concentrations (PPSU 25 %, 29 %, and 30 %). Also, it is well known in the preparation of membranes that if the polymer concentration exceeds 30 wt.% in dope solution results to form membrane with very dense surface without pure water permeation flux as it was observed by using 31 wt.% PPSU in this work. Therefore, 30 wt. % was selected as a highest concentration of PPSU from which it can be obtain the nanofiltration membrane. These hollow fibers were prepared using a phase inversion method with the solvent N-methyl-2--pyrrolidone. The PPSU polymer was dissolved in NMP using magnetic stirrer for 24 h at 40 °C until the mixture was homogeneous. Then, the homogeneous mixture of PPSU-NMP was kept in a cylindrical stainless steel column pressurized under N_2 gas overnight for removal of air bubbles. The PPSU hollow fibers were prepared using dry-wet spinning process using pure water as external coagulant under ambient temperature. The stainless steel spinneret used has 0.9 mm and 0.5 mm outer and inner diameter, respectively. In order to avoid the hollow fiber extension, the take-up speed of the nascent fiber was similar to the falling speed in the external coagulation bath. Then, the nascent PPSU hollow fibers were kept in deionized water for 24 h to remove the residual NMP solvent. Hollow fibers with small and optimal wall thickness

can be formed by increasing the bore fluid flow rate. The suitable flow rate of the bore fluid was found to be 3 ml/min. All the spinning parameters are shown in Table 1, and the hollow fiber fabrication procedure is shown elsewhere in more detail [23–25]. The hollow fiber with PPSU 24 wt.% has a non-dense, selective outer surface and is not suitable for the FO process. Finally, the hollow fibers were moved in a 35 wt% glycerol solution and kept for two days to protect the structure of the membrane from cracking and collapse. Finally, the hollow fiber was kept in air at ambient temperature for drying before the preparation of cell for FO process.

2.3. Membrane characterization

The SEM technique was used to investigate the structures of the cross-section, and inner and outer surfaces of the PPSU fibers. A SEM instrument (TESCAN VEGA3 SB; EO Elektronen-Optik-Service GmbH, Germany) was employed to test the morphological structure of the hollow fibers. To prevent damage to the hollow fiber cross-section structure, the hollow fiber forward osmosis (HFFO) membrane samples were immersed and fractured in liquid nitrogen. An atomic force microscope (AFM) model AA3000 (A. A. Inc., USA), was used to investigate the topography and roughness of the hollow fiber membrane surface under the dynamic mode, which was evaluated using the average surface roughness (Ra), the root mean square roughness (Rq), mean pore size, and pore size distribution.

The HFFO membrane porosity was determined using the volumetric weight for three pieces (each 4-cm long) of each sample of the HFFO membrane, which was measured by an electronic balance. Then, the HFFO membrane porosity was calculated using the following equation [26]:

$$\text{Porosity } (\varepsilon) = \left[1 - \frac{G}{1.41 \times 4}\left\{\frac{4}{(d_{out}^2 - d_{in}^2) \times 10^{-8}\,\pi}\right\}\right] \quad (2)$$

where G is the measured weight of the dried sample of the HFFO membrane. The quantities d_{in} and d_{out} are the inner and outer diameters of the HFFO membranes, which were measured by SEM analysis. The PPSU density was 1.28 g/cm^3.

2.4. Forward osmosis system

The experimental work was conducted using the FO system shown in Fig. 1. The experimental system consisted of two cylindrical, one-liter vessels, the first for the feed solution and the second for the draw solution. Two diaphragm pumps were used to pump the draw and feed solutions from the vessels to the FO module. The hollow fiber module was prepared using a stainless steel tube 24.56 cm in length. PPSU hollow fiber membranes were inserted in the stainless steel tube and sealed with the epoxy resin hardener (Euxit 50 KII). The volumetric flow rates of the feed and draw solutions were measured using two calibrated flow meters in the range of 0.1–1 l/hr. The feed and draw solutions were run in a counter-current flow mode. The operating system in this mode provided a constant osmotic pressure difference ($\Delta\pi$) across and along the membrane module. The outlet streams of the liquids from the osmosis cell were returned to the main vessels of the feed and draw solutions. All experiments using the FO process were carried out at

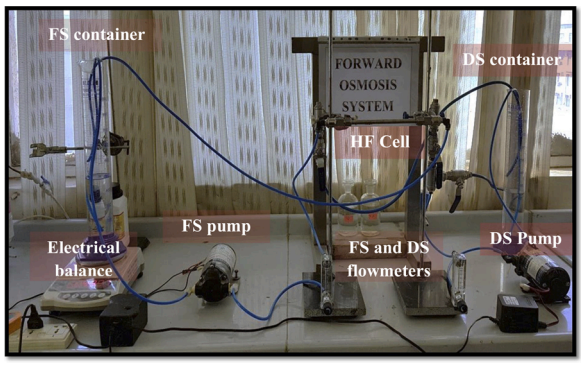

Fig. 1. Experimental bench scale of forward osmosis (FO) system.

atmospheric pressure and at a temperature of 25 ± 5 °C for both solutions. Concentrated NaCl aqueous solutions in the range of 1–3 Molarity (M) were utilized as a draw solution (DS), while 0.5 Molarity (M) NaCl was used as a feed solution (FS). Each experiment ran for 4 h, with the operating conditions of the forward osmosis process summarized in Table 2.

2.5. Measurement of the FO performance

2.5.1. Water permeability coefficient (A)

A pressure-driven permeation test was used to evaluate the HFFO membranes' performance in relation to water permeability. HFFO membranes (24.56-cm long) were installed in the HF module. Then, the inlet pressure of the feed solution was increased from 0 to 2 bar. The FS was forced to permeate from the shell side of the HFFO membrane to the lumen side. The inlet feed solution flow rate was 1.0 l/h. The PWP was measured using DI water. This permeation experiment was carried out at room temperature (25 °C). The results showed that the increase in the pure water flux J_w was linearly correlated with the increase in the transmembrane pressure (TMP, ΔP), as described by the following equation [27]:

$$J_w = A.\ \Delta P \quad (3)$$

where J_w represents the water flux (l/m^2 h), and ΔP is the applied pressure (bar).

2.5.2. Salt rejection (Rs)

One of the most notable characteristics of hollow fiber membranes is their ability to reject salts. Salt rejection (Rs) was obtained by using a feed solution with a 1000 ppm NaCl concentration at 1 bar transmembrane hydraulic pressure. The NaCl concentrations in the feed (C_f)

Table 2
Variables of operating conditions for FO process.

Variables	Ranges
Concentration of draw solution (DS)	1−3 M
Concentration of feed solution (FS)	0.5 M
Flow rate of draw solution (Q_{DS})	0.1−1 l/min
Flow rate of feed solution (Q_{FS})	0.1−1 l/min

Table 1
Spinning parameters of PPSU hollow fiber membranes.

Membrane code	Dope composition PPSU/NMP (wt%)	Bore fluid type	Coagulation bath temperature (°C)	Extrusion pressure (bar)	Bore fluid flow rate (ml/min)	Air gap length (cm)
PPSU-25	(25:75)	Water	36	2.5	3	3.5
PPSU-29	(29:71)	Water	36	2.5	3	3.5
PPSU-30	(30:70)	Water	36	2.5	3	3.5

side and permeate side (C_p) were measured using a conductivity meter, after which the salt rejection (R_S) was evaluated using the following equation [28]:

$$R_s = \left(1 - \frac{C_P}{C_F}\right) \times 100\ \% \quad (4)$$

where Rs is the rejection rate (%), C_P is the concentration of NaCl on the permeate side (mg/l), and C_F is the concentration of NaCl on the feed side (mg/l).

2.5.3. Salt permeability coefficient (B)

The salt permeability coefficient (B) m/s was calculated according to the solution-diffusion theory by a linear fitting based on the following equation [27]:

$$\frac{1 - R_S}{R_S} = \frac{B}{A(\Delta P - \Delta\pi)} \quad (5)$$

2.5.4. The structural parameter (S)

The resistance of the membrane surface to the internal concentration polarization (ICP) effect can be evaluated by calculating the structural parameter of the membrane (S). The structural parameter is a fundamental property of HFFO membranes based on the support layer characteristics: the porosity (ε), tortuosity (τ), and thickness (t) of the membranes, where ($S = t\ \tau\ /\ \varepsilon$). These characteristics can be calculated using Eq. (6), the classical ICP model advanced by [29]:

$$S = \left(\frac{D}{J_W}\right) \ln \frac{B + A\pi_D}{B + J_W + A\pi_{F,m}} \quad (6)$$

where D is the diffusion coefficient of the NaCl ($D = 1.33 \times 10^{-9}$ m/s at 25 °C) [30], π_D the osmotic pressure of the bulk draw solution (DS), and $\pi_{F,m}$ is the osmotic pressure at the surface of the membrane in the)FS(.

For high salt rejection membranes, B is ordinarily assumed to be zero. The structural parameter (S) of the fabricated HFFO membranes was evaluated using a 1.0 M NaCl solution and DI water as the draw and feed solutions, respectively. The flow rate was maintained at 0.1 l/min for both the draw and feed solutions. When utilizing (DI) water as the feed ($\pi_{F,m}$ = zero), Eq. (6) can be simplified to the following [30]:

$$S = \left(\frac{D}{J_W}\right) \ln \frac{A\pi_D}{J_W} \quad (7)$$

2.5.5. Water flux

By determining the volume changes for the feed solution (FS), the flux of the water for the three HFFO membranes can be found using the following equation [27]:

$$J_W = \frac{\Delta V}{\mathrm{Am} \times \Delta t} \quad (8)$$

where J_W represents the water flux (l/m^{2}hr), ΔV represents the volume changes of the feed solution volume (liter), Δt represents the measured time interval (hr), and A_m represents the effective membrane area (m^2).

2.5.6. Solute flux

The reverse solute flux is the diffusion of salt from the draw solution side to the feed side of the membrane. This flux was calculated by the following equation after measuring the volume and the change in the conductivity of the feed solution FS [28]:

$$J_S = \frac{\mathrm{CtVt} - \mathrm{CoVo}}{Am \times \Delta t} \quad (9)$$

where J_S is the salt flux l/m^2 h, Vt is the feed solution volume at time t (liter), Vo is the feed solution volume at time 0 (liter), Ct is the feed solute concentration in the feed tank at time t (g/l), Co is the feed solute concentration in the feed tank at time 0 (g/l), and A_m is the effective area of the membrane (m^2).

3. Results and discussion

3.1. Scanning electron microscope (SEM)

Fig. 2 shows the structural morphology images of the hollow fibers with different PPSU concentrations (i.e., 25, 29, and 30 wt.%). As can be seen from Fig. 2, the structure of the PPSU fibers consists of a dense, selective skin layer at the outer surface; a sponge-like structure extended in the direction of the inner surface (lumen side) to a short layer, which consists of few and small finger-like macrovoids; and an inner skin layer with a porous structure. The formation of a dense skin layer is attributed to the immediate phase separation during the fiber formation because of a huge amount of a strong non-solvent (water) as an external coagulant. In contrast, the formation of a sponge-like structure is attributed to the retarded NMP-water diffusion rate induced by the NMP enriched with very low amounts of a water internal coagulant [23–25,31–33]. Also, from Fig. 2 it can be clearly observed from the inner surface that the pores size of the PPSU hollow fibers prepared from 30 wt.% were smaller than other two PPSU fibers. The sublayer for 30 wt.% of PPSU is composed of sponge-structure with thin micro-voids appeared at the edge of the inner surface. Whereas the sublayer of hollow fiber prepared from 29 wt.% PPSU was composed of large and wide micro-voids. This is means that increasing of polymer concentration in dope solution from 29 to 30 wt.% results to reduce the size of the micro-voids and willing to change these micro-voids to fully sponge structure. The predominant sponge-like structure produces a PPSU fiber with high mechanical properties, which in turn overcomes the high transmembrane pressure of the NF process.

3.2. Parameters affecting membrane performance

3.2.1. Porosity and thickness

Table 3 illustrates the change in porosity values for the three HFFO membranes as a function of polymer concentration (PPSU 25 %, 29 %, and 30 %). The PPSU fiber with 25 % showed higher porosity (i.e., 83.72 %) than the others, with a porosity of 82.45 % and 79.87 % for PPSU 29 % and 30 %, respectively. Increasing the polymer percentage in the dope solution reduced the membrane porosity, which agrees well with the results of previous studies [27,34]. Moreover, in Table 3, it can be observed that the thickness of the PPSU 25 % HFFO membrane was small compared with the thickness of the membranes for PPSU 29 % and PPSU 30 %. It has been established that the membrane thickness increases with an increase in the polymer percentage [34]. A thin membrane is a preferred parameter for high permeation flux across the membrane due to its lower resistance to permeation flux. In addition, it is expected that with greater membrane thickness, more impact of the internal concentration polarization (ICP) development that results in reducing the driving force and thus decreasing the permeate flux rate [35]. Hence, a thin membrane is optimal for the purpose of minimizing the ICP. Therefore, reducing the thickness of the membranes, as was prepared by this work (i.e., 57.01∼65.56 μm), effectively minimizes the transport resistance and internal concentration polarization (ICP) and makes the membrane more suitable and efficient for FO process performance.

In Table 3, the resulting hollow fibers composed of a thin skin layer about 0.5 μm in thick (perm-selective layer), for hollow fiber prepared from 25 wt. % of PPSU, while the thickness of the 29 and 30 wt.% PPSU fibers was 0.91 and 0.96 μm, respectively. In fact, increasing the polymer concentration in the dope solution was resulting in the increasing of the thickness of the skin layer of the hollow fibers [31,33].

3.2.2. Structural parameter (S)

The membrane structural parameter is an intrinsic, essential property that shows the extent to which the membrane is affected by the

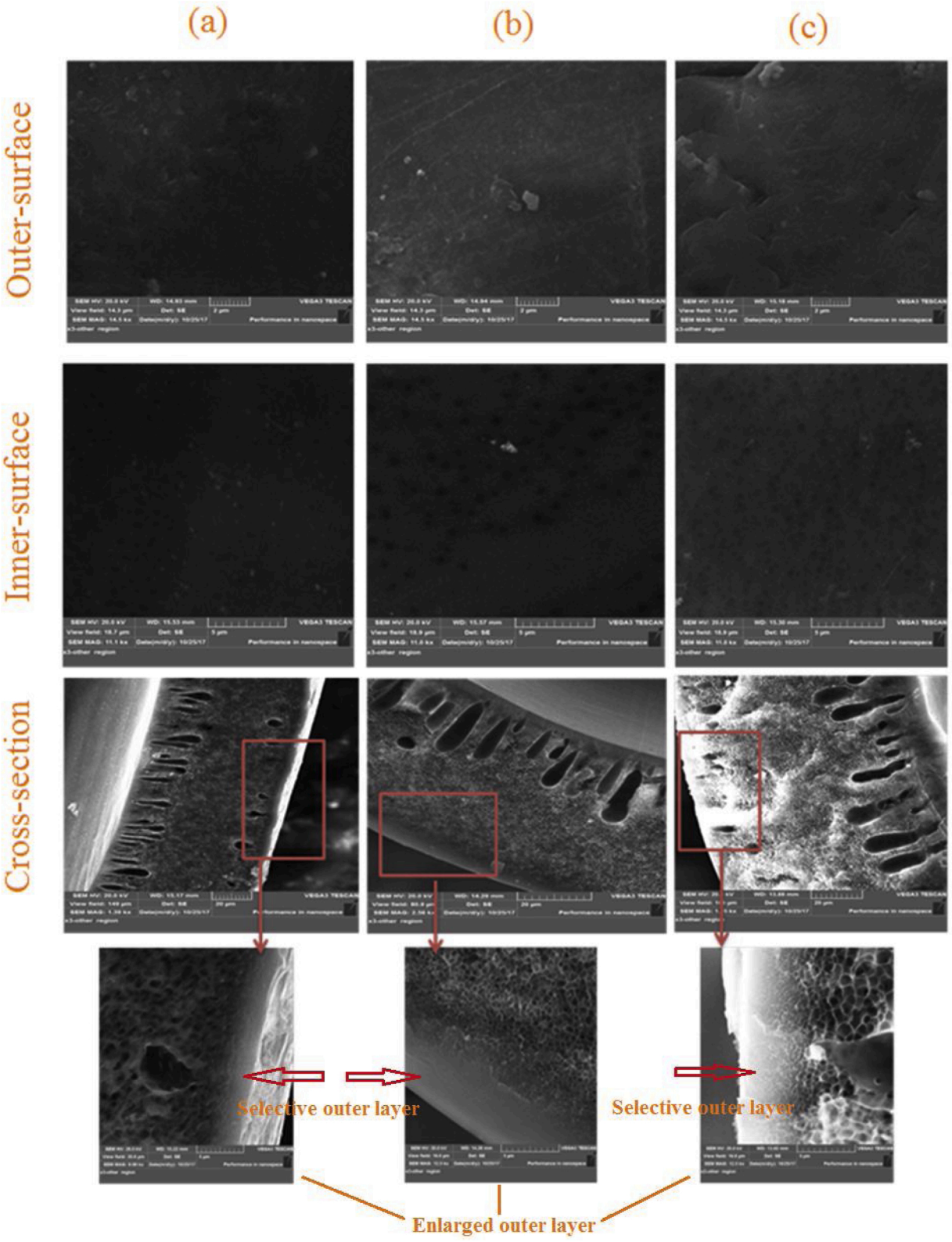

Fig. 2. The hollow fibers SEM images with different PPSU concentrations: (a) 25 wt %, (b) 29 wt %, (c) 30 wt %.

internal concentration polarization. In FO, a low value of the structural parameter indicates positive performance mainly because this reduces the tortuosity according to the following: $S = t\ \tau/\varepsilon$. Experiments using the FO test apparatus were employed to calculate *S*, using the protocol described in earlier studies [36,37]. As shown in Table 3, the increase in the water flux for PPSU 25 % can be attributed to the decrease in the structural parameter (S value = 467 μm), whereas other hollow fibers (i.e., PPSU with 29 and 30 wt.%) had the relatively high S values of 567 and 601 μm, respectively. In short, based on the performance results of the three PPSU hollow fibers, an increase in the structural parameter (S) has been confirmed to contribute to a lower water permeation flux [38]. Therefore, it can be concluded that the structural parameter is a

Table 3
Summary of the calculated transport parameters A, B, R_S and S, with porosity, and length for three hollow fiber membranes.

Sample membranes	Length (cm)	Thickness (μm)	Porosity ε (%)	Skin layer thickness (μm)	Water permeability coefficient, A [LMH/bar]	Salt permeability coefficient, B [LMH]	Salt rejection R_S (%) at 1 bar	Structural parameter (S) (μm)
PPSU 25 %	24.56	57.01 ± 0.73	85.72 ± 0.98	0.5	2.25	0.371	85.1	467
PPSU 29 %	24.56	62.61 ± 1.08	82.02 ± 0.71	0.91	1.59	0.250	86.2	567
PPSU 30 %	24.56	65.56 ± 0.69	79.55 ± 0.82	0.96	0.99	0.105	89.8	601

reasonable parameter for evaluating hollow fiber efficiency.

3.3. Water permeability coefficient (A), salt rejection (Rs), and salt permeability coefficient (B)

The pure water permeability (PWP) for the three types of membranes was measured using a cross-flow filtration system by applying trans-membrane pressure (TMP, ΔP) from 0 to 2 bar and using DI water as a feed solution. As shown in Table 3, the PPSU 25 % membrane showed a PWP value (2.25 LMH/bar) higher by 29 % and 56 %, respectively, than for PPSU 29 % (PWP 1.59 LMH/bar) and PPSU 30 % (PWP 0.99 LMH/bar). These results are clearly due to the fact that water permeability increases with decreasing polymer content and thickness (fiber wall resistance) [31,33].

The salt rejection of the membranes tested at room temperature, 1.0 bar transmembrane pressure, and a 1000-ppm NaCl solution was used as a feed, as suggested in Zhong et al. [38]. As shown in Table 3, the three membranes exhibited various levels of salt rejection of NaCl, where PPSU 25 % showed the smallest rejection (i.e., 85.1 %) among the hollow fibers tested. PPSU 30 % had the higher salt rejection (Rs) (i.e., 89.9), by about 5.5 % and 4%, in relation to PPSU 25 % and PPSU 29 %, respectively. These results were expected because increasing the polymer concentration in the dope solution leads to an increase in the thickness of the fiber wall due to the increase in the amount of solid material in the dope solution. This, in turn, increases the water permeation resistance and high solute rejection. Also, increasing the amount of solid material in the dope solution decreases the porosity of the fibers and reduces the fiber pore size, also leading to a high solute rejection. Therefore, hollow fibers with a higher rejection can reduce the salt reverse flux in the FO process [33].

The salt permeability coefficient (B) represents an intrinsic property of a membrane, and it was found based on the solution-diffusion theory [36]. PPSU 25 % showed a higher salt permeability coefficient (B) of about 0.371 LMH in comparison to PPSU 29 % (0.250 LMH) and PPSU 30 % (0.105 LMH).

3.4. Effect of operating conditions

3.4.1. Flux variation with time

As shown in Fig. 3, the PPSU 25 % membrane showed a much higher water flux than either the PPSU 29 % or PPSU 30 % membranes. In general, it can be observed that all three membranes showed a water flux decline with time during the test. There was a great decline in the water flux after the first half hour of the experiment to about 24 % for PPSU 25 % and PPSU 29 %, compared to 22 % for PPSU 30 %. The amount of reduction in the water flux decreased over time. The flux difference among these membranes was due to the PPSU polymer content, which in turn affected the polymer solution properties. The PPSU 25 % membrane thickness was 57.01 μm, which was less than the thickness of either the PPSU 29 % or PPSU 30 % membranes, which measured 62.61 and 65.56 μm, respectively. That explains the thick support layers of the PPSU 29 % and PPSU 30 % membranes, which may influence the development of the internal concentration polarization (ICP) and might also reduce the effective driving force of the process, and hence, of the water flux [39].

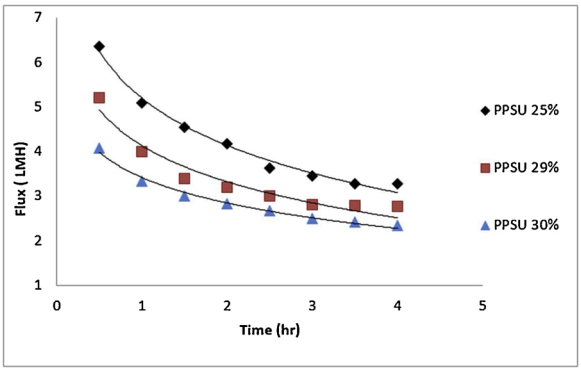

Fig. 3. Water Flux Change with time (Temp. 25 ± 5 °C, DI water & 1 M draw solution concentration 0.1 l/m feed & draw solution flow rate, for three type of PPSU HF Membrane).

3.4.2. Effect of the draw solution concentration on the water flux

The water fluxes at different draw solution concentrations (1.0–3.0 M NaCl) were measured, as shown in Fig. 4. This figure displays increases in the water flux with increasing draw solution concentrations. This is due to increasing the effective osmotic driving force across the HFFO membranes while also increasing the draw solution concentration. The osmotic pressure difference ($\Delta\pi$) is the driving force in the FO process. This event is symptomatic of the beginning of the ICP in the porous substrate layer, which it is very sharp in FO fibers. These results were confirmed by several studies presented in the literature [40–42]. Fig. 4 illustrates that some deviation from the linearity was observed due to the effect of the ICP [43].

3.4.3. Effect of the draw solution flow rate on the water flux

Fig. 5 presents the effect of the draw solution flow rate (Q_{DS}) on the water flux at the same concentration of the draw solution (1.0 M) for the three types of HFFO membranes. The results show that increasing the DS flow rate adversely affected the flux, which occurred because of the increased accumulation of concentrated salt at the membrane surface, which reduced the driving force required for water transfer. For PPSU 25

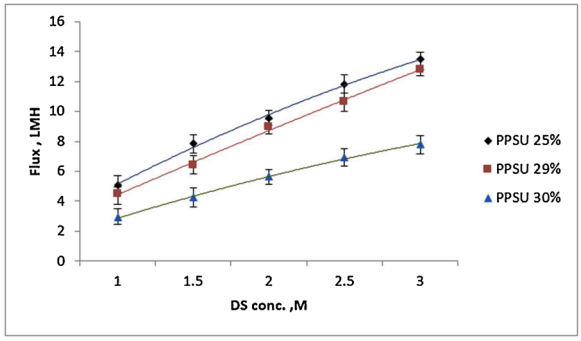

Fig. 4. Water Flux Change with Draw Solution Concentration (Temp. 25 ± 5 °C, Feed & Draw Flow Rate 0.1 l/min, 0.5 M FS concentration, for three types of PPSU Membranes).

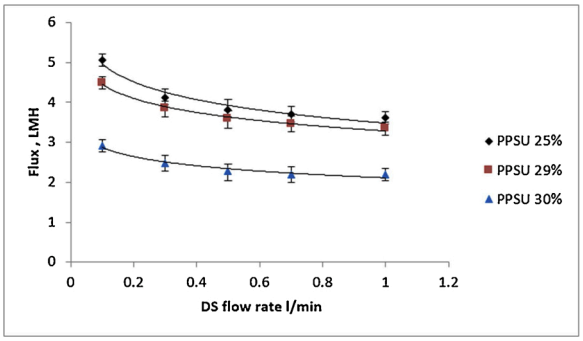

Fig. 5. Water Flux Change with DS flow rate (Temp. 25 ± 5 °C, 0.5 M feed solution conc. & 1 M draw solution conc., 0.1 l/m feed solution flow rate, for three types of PPSU Membranes).

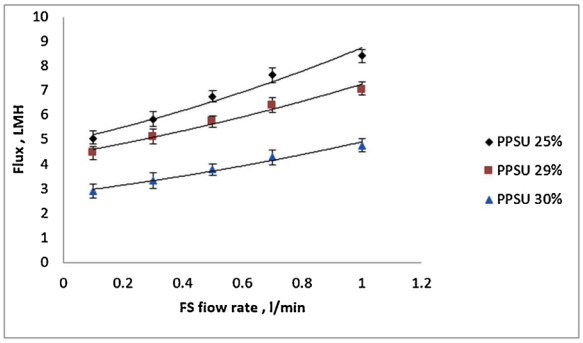

Fig. 6. Water flux change with FS flow rate (Temp. 25 ± 5 °C, 0.5 M Feed solution conc. & 1 M draw solution conc., 0.1 l/m draw solution flow rate, for three types of PPSU Membranes).

%, 29 %, and 30 % membranes, the decrease in the water flux with the draw solution flow rate of 0.1−0.5 l/min was approximately 24 %, 20 %, and 21 %, respectively, and for the flow rate of 0.5−1.0 l/min was 5.2 %, 6%, and 3.9 %, respectively. Fig. 5 shows decreases in the water flux with the draw solution flow rate (Q_{DS}) and that PPSU 30 % was the least affected of the hollow fibers. Increasing the flow rate of the DS on the support layer of the HFFO membranes had no effect on reducing the ICP.

3.4.4. *Effect of the feed solution flow rate on the water flux*

The effect of different feed solution flow rates (Q_{FS}) (i.e., 0.1, 0.3, 0.5, 0.7, and 1.0 L/ min) on the permeate flux for the three types of HFFO membranes is shown in Fig. 6. For the PPSU 25 % membrane, there was a percentage increase in the water flux with the feed flow rate of 0.1−0.5 l/min, from 5.05–6.74 LMH, with the flux increasing from

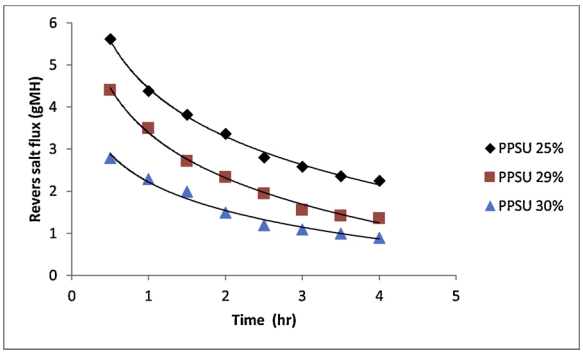

Fig. 7. Reverse Salt Flux with Time (Temp. 25 ± 5 °C, DI water of feed solution & 1 M draw solution conc., 0.1 l/min feed & draw solution flow rate, for three types of PPSU HF Membranes).

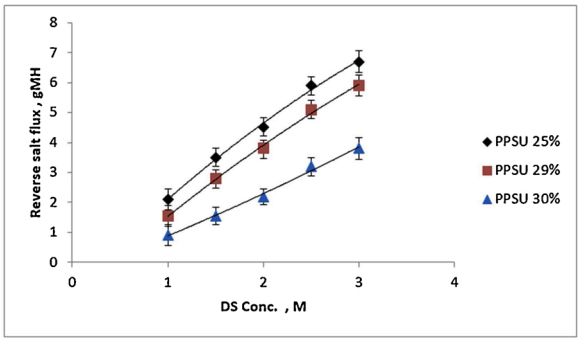

Fig. 8. Effect of Draw solution concentration on the reverse salt flux (Temp. 25 ± 5 °C, Feed & Draw Flow Rate 0.1 l/min, 0.5 M FS conc. and for three types of PPSU Membranes).

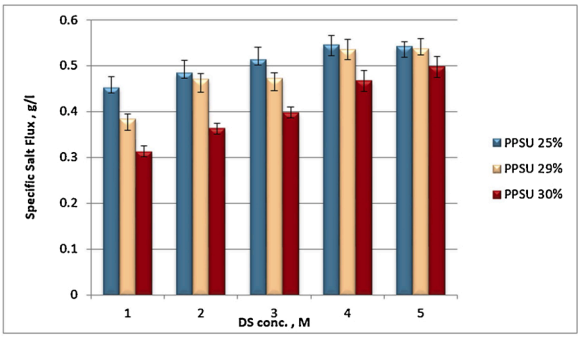

Fig. 9. Comparison of Specific Reverse Salt Flux with Different concentration of Draw Solutions for three types of membranes (Temp. 25 ± 5 °C, Feed & Draw Solution Flow Rate 0.1 l/min and 0.5 M FS concentration).

6.74 to 8.42 LMH for the feed flow rate of 0.5−1.0 l/min. For the PPSU 29 % and PPSU 30 % hollow fibers, the increase in the water flux for the flow rate of 0.1−0.5 l/min was from 4.48 to 5.76 LMH and from 2.90 to 3.81 LMH, respectively. Moreover, when the flow rate increased to 0.5−1.0 l/min, the water flux increased from 5.76 to 7.05 LMH for PPSU 29 % and from 3.81 to 4.76 LMH for PPSU 30 %. These results prove that the PPSU 25 % membrane is preferable to the others. Also, it can be seen from Fig. 6 that the PPSU 30 % membrane was less influenced by Q_{FS} variation because the increase in the water permeate flux is proportional to increases in the FS flow rate. Increasing the flow rate of the FS lowered the accumulation of the solute concentration near the active layer of the HFFO membrane surface (i.e., reducing the concentrative external concentration polarization). This decreased the osmotic pressure in the

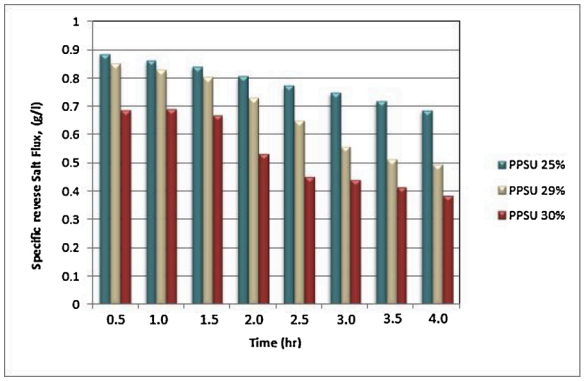

Fig. 10. Specific reverse salt flux with Time (Temp. 25 ± 5 °C, DI water & 1 M draw solution concentration, 0.1 l/m feed & draw solution flow rate, for three types of PPSU HF Membranes).

Table 4
For various types of membranes, operating conditions and performance were obtained in several studies for FO.

Membrane	Feed solution	Draw solution	Water flux (LMH)	Revers salt flux (gMH)	FS flow rate	DS flow rate	Temp.	Water permeability coefficient (A) [LMH/bar]	Salt permeability coefficient (B) [LMH]	Membrane porosity ε %	Structural parameter (S)	Salt rejection (%)	Ref.
PPSU 25 % HF	0.5 M	3 M	13.48	7.30	0.1 L/min	0.1 L/min	25 ± 5°C.	2.25	0.37	85.72	467 μm	85.1	[This work]
PPSU 29 % HF	0.5 M	3 M	12.82	6.58	0.1 L/min	0.1 L/min	25 ± 5°C.	1.59	0.25	82.02	567 μm	86.2	[This work]
PPSU 30 % HF	0.5 M	3 M	7.81	3.89	0.1 L/min	0.1 L/min	25 ± 5°C.	0.99	0.99	79.55	601 μm	89.8	[This work]
PPSU (non-sulfonated) HF	DI water	2 M NaCl).	10	2.3	8.33 cm/s	8.33 cm/s	22 ± 0.5°C.	6529	5.78	65	2.94×10^{-3} m	81.71	[42]
TFC PPSU	DI water	0.5 M NaCl	12.37 ± 1.2	2.69 ± 0.21	0.1 L/min	0.2 L/min	23 °C	3.15 ± 0.07	0.0952 ± 0.003	_	7.46×10^{-4} m	86.8 ± 0.7	[38]
TFC polyketone HF-B	DI water	Sodium chloride 0.05−1.o M	_	_	1.0 L/h	1.0 L/h	25 ± 5°C.	_	_	_	_	93	[48]
CA with an acylation degree of 39.2 %	0.2 M NaCl	1.5 M glucose	3.47	_	0.33 m/sec,	0.33 m/sec,	25 °C	_	_	_	_	95.48	[51]
(CA) nanofiltration HF	saline water	2.0 M MgCl2	7.3	0.53	50 mL/min	100 mL/min	25 °C	0.47	_	_	_	90.17	[46]
PVDF/PFSA TFC (MT-0)	DI water	1 M NaCl	2.5	12.0	0.3 L/min	0.3 L/min	ambient temperature	0.11 ± 0.01	0.93 ± 0.02	72.4 ± 0.3	1606.51 ± 37.31 μm	15.18 ± 0.29	[50]
Dope formula A (PES) single skinned	DI water	0.5 M NaCl	5	2.12	_	_	23 °C.	0.95	0.29	84	1.37 × 10 − 3 m	78	[41]
PES/SPSf TFC FO	DI water	0.5 M NaCl	13.0	3.6	100 mL/min	100 mL/min	20–25 °C	0.77	0.11	83.3	2.38 × 10 − 4 m	93.5	[18]
PBI hollow fiber (original) in PRO mode	DI water	5 M MgCl2	36.5	_	_	0.08 m/s	23 °C	2.43	_	_	_	_	[53]
ST#3 PAI hollow fiber	DI water	0.5 M MgCl2	12.9	4.773	450 mL/min	1500 mL/min	23 °C	2.19	0.138	85	_	91.1	[54]
TFC PK(25/75) (70)-1	DI water	0.6 M NaCl	13.8	0.047	500 mL/min	500 mL/min	25 ± 2°C	1.21	0.2	_	364 μm	_	[55]
SPPO/PSf (50:50)	DI water	1.0 M MgCl2	29 ± 3	1.4 ± 0.2	0.26 L/min	0.26 L/min	25°C	3.55	0.74	86	293 ± 22 μm		[56]
hydrophilic cellulose-based polymer (CA)	sodium chloride	ammonia–carbon dioxide	3.6 – 36..0	–	30 cm/s	30 cm/s	50 ± 1 °C	$5.69\times10-12$ $mPa^{-1}\ s^{-1}$	–	–	–	95–99	[16]
(PES) hollow fiber	DI water	0.5 M NaCl	42.6	4.0	–	–	23 °C	3.50	6.22 × 10 − 8 m/s	82	5.50 × 10 − 4 m	~95	[57]
TFC (Sulphonated polyethersulfone (SPES))	DI water	2.0 M NaCl	35	9.9	200 mL/min	200 mL/min	25°C	2.9 ± 0.25	5.1 ± 0.1.3	79 ± 3	245 μm	91.1	[58]
Polyamide (PA) & polysulfone (TFC) membrane	5 g/L	2.5 M ammonium sulphate	21.67	–	400 mL/min	400 mL/min	25 °C	3.036	1.968	–	–	85.2	[59]
The thin film nanocomposite TFN0.5	10 mM NaCl	2M NaCl	27.7	14.62	0.35 L/min	0.35 L/min	0.35 L/min	2.00	9.34	77 ± 0.45	0.37 ± 0.05	93.7	[60]
Cellulose triacetate (CTA)	DI water	1 M Fertilizers (f1)	4.2	–	10 to 100 mL min^{-1}	10 to 100 mL min^{-1}	20 ± 2 °C	0.6−1.0	–	–	–	81	[61]
			1.4	–	–	–	–	–	–	–	–	60−70	[41]

(*continued on next page*)

Table 4 (*continued*)

Membrane	Feed solution	Draw solution	Water flux (LMH)	Revers salt flux (gMH)	FS flow rate	DS flow rate	Temp.	Water permeability coefficient (A) [LMH/bar]	Salt permeability coefficient (B) [LMH]	Membrane porosity ε %	Structural parameter (S)	Salt rejection (%)	Ref.
FO flat sheet membrane	32,500 ppm Surface seawater	1.15 M Sodium sulphate											
polysulfone/ polyacrylonitrile (PSf/PAN) nanofibers	DI water	79.27 g/L KCl	38.3	10.1	–	–	25 °C	3.68 ± 0.23	0.32 ± 0.12	84.3	0.34 mm	97.12 ± 0.92	[62]

feed solution region, resulting in an increased driving force, which increased the water flux. These observations agree well with those reported by [44], which stated that the flux declined with a lower FS flow rate due to the ECP, which is limited by the flow velocity.

3.4.5. Reverse salt flux variation with time

Fig. 7 shows the difference in the reverse salt flux during the FO operation for the three types of HFFO membranes at a temperature of 25 ± 5 °C, DI water as a feed solution, 1 M as a draw solution concentration and 0.1 l/min of feed and draw solution flow rate. The reverse salt flux decreased during the time of operation. For the PPSU 25 % membrane, the decrease was 21 % after the first half hour of the FO operation, while for the PPSU 29 % and PPSU 30 % membranes, the decrease was 20 % and 17 %, respectively. The decrease in the reverse salt flux was severe only in the first two hours of operation. This difference was mainly due to the structure of the hollow fibers. Fibers with high polymer concentration may constrict the pore size, which in turn minimizes the reverse salt flux. After two hours of operation, the sharp reduction in the reverse salt flux decreased due to the reduction in the draw solution concentration with time (diluted by the water flux). This reduced the driving force for the mass transfer between the draw solution side and the feed solution side so that the reverse diffusion of salt from the draw solution to feed solution decreased with time.

3.4.6. Reverse draw solute flux as a function of the draw solution concentration

To study the effect of the draw solution concentration on the reverse solute flux, several experiments were conducted using NaCl (known as sodium chloride or salt) with different concentrations; for example, from 1–3 M for the three types of HFFO membranes. The results of the experiments are shown in Fig. 8. The highest reverse salt flux (RSF) was obtained for PPSU 25 %. The increase in the reverse salt flux for PPSU 25 % was 67 % for concentrations from 1.0–1.5 M, while the RSF was 80 % and 70 % for PPSU 29 % and PPSU 30 %, respectively. The increase in the salt flux with increases in the NaCl concentration from 2.0–3.0 M were 78 %, 55 %, and 18 % for PPSU 25 %, 29 %, and 30 %, respectively. As expected, increasing the concentration of the draw solution increased the reverse solute flux as a result of increasing the driving force for the mass transfer between the draw and feed solutions as in the previous research of Al-aibi et al. and Phillip et al. [45,46]. Their studies showed that the reverse salt flux (Js) increased with an increase in the osmotic pressure difference (i.e., an increase in the sodium chloride draw solution concentration).

3.4.7. Specific reverse salt flux (SRSF) with draw solution concentration and operation time

The specific reverse salt flux (SRSF, Js/Jw) measurement is an essential and well-known method for assessing the performance of a membrane and the draw solution. The specific reverse salt flux measurements for the draw solutions used in this study are displayed in Fig. 9, where Js represents the reverse salt flux, and Jw represents the water flux. The average Js/Jw for PPSU 25 %, 29 %, and 30 % was 0.5, 0.47, and 0.40 g/l, respectively. The PPSU 25 % had a higher Js/Jw than either the PPSU 29 % or PPSU 30 %. The SRSF is used to evaluate the lost quantity of the draw solute during the FO process for each liter of water generated. As can be seen in Fig. 9, the increase in the SRSF for all the PPSU fibers, which occurred along with increases in the draw solution concentration, was attributed to the concentration polarization and concentration gradient being at a higher concentration of the draw solution [47].

Fig. 10 shows the variations of the SRSF with time for fibers used for FO membranes when employing a high DS concentration of 1 M NaCl and deionized water (DI) as an FS. The results indicate a reduction in the specific RSF during the FO operation due to decreases in the draw solution concentration with time. This reduced the reverse salt flux from the draw solution in comparison to the water flux and also because of the

Table 5
A comparison of the three PPSU fibers performance fabricated in this work with different commercial membranes presented in the literature.

Commercial Membranes	Feed solution	Draw solution	Water flux (LMH)	Revers salt flux (gMH)	Structural parameter (S) (μm)	Solute rejection (%)	Ref.
TFC, polyamide (Porifera Inc., USA)	Digester centrate	Seawater	5		215	phosphorus <(96)	[63]
TFC membrane (polyamide as selective layer) (Aquaporin A/S, Denmark)	DI	1.0 M NaCl	8.8	10	569		[64]
HTI CA polyamide selective layer membranes	DI	1.0 M NaCl	9	7.5	–		[64]
Polyamide (PA) & polysulfone (TFC) membrane, supplied by Hydration Technology Innovations (HTI), LLC, Albany, Oregon, USA	5 g/L	2.5 M ammonium sulphate	21.67		–	85.2	[59]
TFC-ES, the semi-permeable membranes used were acquired from Hydration Technology Innovation (HTI) and Porifera	Distilled water	1.0 M NaCl	17			99.4	[44]
ACT-Es, cellulose triacetate, the semi-permeable membranes used were acquired from Hydration Technology Innovation	Distilled water	1.0 M NaCl	9.3			99.2	[44]
Cellulose triacetate, DURASEP-FO-AC (Toyobo Ltd)	DI	0.841 M NaCl	3.5			91.04 ± 0.15	[45]
TFC membrane was supplied by Hydration Technology Innovations (Albany, Oregon, USA)	DI	1 M ethylenediaminetetraacetic acid (EDTA-2Na)	8.8	9	–	94.8 ± 0.17	[47]
PPSU 25 % HF	DI	3 M	13.48	7.30	467	85.1	This work
PPSU 29 % HF	DI	3 M	12.82	6.58	567	86.2	This work
PPSU 30 % HF	DI	3 M	7.81	3.89	601	89.8	This work

concentration polarization that could take place during the FO operation. Hollow fiber prepared from PPSU 25 % showed higher J_s/J_w (0.88 g/l) than PPSU 29 % (J_s/J_w =0.84 g/l) and PPSU 30 % (J_s/J_w =0.68 g/l) after the first half hour of the FO experiment. At four hours, the J_s/J_w for PPSU 25 %, 29 %, and 30 % were 0.78, 0.67, and 0.52 g/l, respectively. This phenomenon was due to the morphological structure of the hollow fiber surface, which was in contact with the draw solution. Increasing the amount of PPSU decreased the pore size of the fibers, which in turn, lowered the SRSF. The SRSF was a key parameter in the FO because it provided a quantitative measure of the mass of solutes lost from the DS per volume of water recovered from the feed. Therefore, reducing the pore size of the fiber surface during the formation of the hollow fiber by using optimum spinning parameters is recommended. The optimum pore size should be as small as possible to minimize the SRSF phenomenon.

The optimum conditions to fabricate a better FO membrane are the conditions that provide a lower specific reverse salt flux (SRSF) which means a higher water flux and a lower reverse salt flux. This can be achieved by controlling the fabrication conditions of the membrane such as polymer concentration, bore fluid flow rate and extrusion pressure. The ideal FO membranes should have small pore size, thin and porous support layer, and more hydrophilic character of the membrane surface. These characteristics can minimize the effect of concentration polarization and provide higher performance in terms of water flux. In the present work, the optimum conditions for FO membrane fabrication was with hollow fiber prepared from 30 wt.% PPSU, which was selected based on the specific reverse salt flux (SRSF), because this parameter is a key factor in the FO process. SRSF provided a quantitative measure of the mass of solutes lost from the DS per volume of water recovered from the feed. Moreover, it can be conclude from the results presented in the current work that the key factor for better FO performance with minimum SRSF was the pore size of the hollow fiber. Therefore, reducing the pore size of the hollow fiber throughout the fabrication process by increasing the PPSU concentration minimizes the SRSF phenomenon.

3.5. Comparison of the FO performance with previous research

To illustrate the effect of the polymer concentration on the properties of the membranes used in the forward osmosis process, this work investigated a new approach to fabricating hollow fiber membranes by using a high percentage (i.e., up to 30 %) of poly(phenyl sulfone) (PPSU), which to the best of our knowledge was not previously used for this purpose. Therefore, a comparison between various membranes selected from the literature prepared from various polymeric materials and reported in the current work is depicted in Table 4. The hollow fiber membranes prepared from PPSU with concentrations of 25 % and 29 % in this work showed higher water flux and salt rejection than other PPSU flat sheet membranes used in the FO and RO mode in a previous study [42], with a much lower salt permeability coefficient (B). In spite of the lower water flux of PPSU 30 % compared with the PPSU hollow fiber membranes used by [38], PPSU 30 % exhibited a higher rejection of salt and lower structural parameters, which are a good indication of the membrane's ability to be resistant to internal concentration polarization. And when discussing the other HF membrane properties as compared with the membranes fabricated by different materials, such as polyketone, as reported in the literature [49], the three PPSU hollow fiber membranes are less thick, which reduces the accumulation of salts on the surface of the membranes. Additionally, PPSU 30 % had a higher water permeability coefficient and lower salt permeability coefficient than the TFC-FO (HF-B) used by [48]. However, in the FO process, the small diameter produced a higher water flux in comparison with [49], which used a large lumen with an inner diameter of > 1 mm and a wall thickness of 0.17–0.215 mm. Moreover, Table 5 shows a comparison of the three PPSU hollow fibers performance fabricated in this work with different commercial membranes presented in the literature. The most significant results of the commercial membranes such as feed solution, draw solution, water flux, revers salt flux, structural parameter (S) and solute rejection are presented in Table 5. It can be noticed that the three PPSU NF hollow fibers exhibit a values of the water flux, reverse salt flux and solute rejection that converged with almost all of the commercial membranes described in the pertinent researches found in the literature. In Table 5 it was clearly noticed the capability of the PPSU NF hollow

fibers to achieve well in the forward osmosis process for application of saline water desalination.

With the variation in the polymer concentration used in the manufacture of the membranes in this research, it can be observed that a low polymer content led to improved properties and performance of the membranes in most respects. Zhang et al. [50] used concentrations ranging from 16−21 wt.% of polyvinylidene fluoride (PVDF), which exhibited a reduced reverse salt flux and an improvement in the membrane performance in porosity, water and permeability coefficients, structural parameters, and water flux. The PPSU-HFFO membranes showed a higher porosity and lower structural parameter (S) as well as a higher water flux than the PVDF 21 % HF membrane despite using a higher PPSU polymer concentration. Most of the research in the field of membrane testing and its efficiency in the forward osmosis process was limited to the use of distilled water as a feed solution [51,52]. The use of synthetic saline water in this work simultaneously gives a practical application of membrane efficiency as well as to the efficiency of the forward osmosis process for optimal saline water desalination.

4. Conclusions

This work has proved that the NF hollow fibers at different PPSU amounts with a dense, selective, outer surface layer can be effectively utilized as FO fibers. The prepared PPSU fibers exhibited an attractive PWP and a high salt rejection. For concentrations of feed solutions and pure water recovery, the PPSU NF fibers are of notable potential to be used in the FO process. The structural parameter (S = 467–601) displayed small values for the three PPSU fibers due to their high porosity and thinness. The new FO PPSU fibers prepared in the current work can realize a desirable salt rejection of between 85.1 and 89.8 %, with a PWP between 7.81 and 13.48 LMH for a 3 M NaCl draw solution and 0.5 M FS concentration. Also, it can be concluded that reducing the pore size of the fiber surface during the formation of the hollow fiber by increasing the PPSU concentration minimizes the SRSF phenomenon. From these results, it can be concluded that the PPSU fibers prepared by this work are promising for the desalination of saline water using the FO process.

CRediT authorship contribution statement

Mariam J. Jaafer: Data curation, Formal analysis, Software, Writing - original draft. **Jenan A. Al-Najar:** Conceptualization, Investigation, Supervision, Writing - review & editing. **Qusay F. Alsalhy:** Conceptualization, Formal analysis, Investigation, Methodology, Resources, Supervision, Validation, Writing - original draft, Writing - review & editing.

Declaration of Competing Interest

The authors report no declarations of interest.

References

[1] S. Xiong, J. Zuo, Y.G. Ma, L. Liu, H. Wu, Y. Wang, Novel thin film composite forward osmosis membrane of enhanced water flux and anti-fouling property with N-[3-(trimethoxysilyl) propyl] ethylenediamine incorporated, J. Membr. Sci. 520 (2016) 400–414.

[2] P. Zhao, B. Gao, Q. Yue, H.K. Shon, The performance of forward osmosis process in treating the surfactant wastewater: the rejection of surfactant, water flux and physical cleaning effectiveness, Chem. Eng. J. 281 (2015) 688–695.

[3] N.Q. Trung, P.T.P. Thao, Novel draw solutes of iron complexes easier recovery in forward osmosis process, J. Water Reuse Desalin. (2017) jwrd2017150.

[4] E. Arkhangelsky, F. Wicaksana, S. Chou, A.A. Al-Rabiah, S.M. Al-Zahrani, R. Wang, Effects of scaling and cleaning on the performance of forward osmosis hollow fiber membranes, J. Membr. Sci. 415 (2012) 101–108.

[5] R.V. Linares, Z. Li, S. Sarp, S.S. Bucs, G. Amy, J.S. Vrouwenvelder, Forward osmosis niches in seawater desalination and wastewater reuse, Water Res. 66 (2014) 122–139.

[6] H.J. Krishna, Introduction to desalination technologies, Texas Water Dev. 2 (2004).

[7] J.T.M. Linders, Patai's 1992 guide to the chemistry of functional groups, S. Patai, John Wiley, Chichester, Recl. Des Trav. Chim. Des Pays-Bas 111 (10) (1992) 458.

[8] H.K. Shon, S. Vigneswaran, J. Kandasamy, J. Cho, Water and wastewater treatment technologies-membrane technology for organic removal in wastewater. Encyclopedia of Life Support System (EOLSS), 2002.

[9] A.F. Al-Alawy, Forward and reverse osmosis process for recovery and re-use of water from polluted water by phenol, J. Eng. 17 (4) (2011) 912–928.

[10] M.A. Darwish, H.K. Abdulrahim, A.S. Hassan, A.A. Mabrouk, A.O. Sharif, The forward osmosis and desalination, Desalin. Water Treat. 3994 (2014) 1–27.

[11] A.H. Hawari, N. Kamal, A. Altaee, Combined influence of temperature and flow rate of feeds on the performance of forward osmosis, Desalination 398 (2016) 98–105.

[12] Q. Ge, M. Ling, T.S. Chung, Draw solutions for forward osmosis processes: developments, challenges, and prospects for the future, J. Membr. Sci. 442 (2013) 225–237.

[13] B.D. Coday, T.Y. Cath, Forward osmosis: novel desalination of produced water and fracturing flowback, J. AWWA (2014) E55–E66.

[14] F.C. Kramer, R. Shang, S.G.J. Heijman, S.M. Scherrenberg, J.B. van Lier, L. C. Rietveld, Direct water reclamation from sewage using ceramic tight ultra- and nanofiltration, Sep. Purif. Technol. 147 (2015) 329–336.

[15] J. Korenak, S. Basu, M. Balakrishnan, C. Hélix-Nielsen, I. Petrinic, Forward osmosis in wastewater treatment processes, Acta Chim. Slov. 64 (2017) 83–94.

[16] Z.X. Low, Q. Liu, E. Shamsaei, X. Zhang, H. Wang, Preparation and characterization of thin-film composite membrane with nanowire-modified support for forward osmosis process, Membranes 5 (1) (2015) 136–149.

[17] J.E. Kim, S. Phuntsho, F. Lotfi, H.K. Shon, Investigation of pilot-scale 8040 FO membrane module under different operating conditions for brackish water desalination, Desalin. Water Treat. 53 (10) (2015) 2782–2791.

[18] K.Y. Wang, T.S. Chung, G. Amy, Developing thin-film-composite forward osmosis membranes on the PES/SPSf substrate through interfacial polymerization, AIChE J. 58 (3) (2012) 770–781.

[19] A. Altaee, G. Zaragoza, H.R. van Tonningen, Comparison between Forward osmosis-reverse osmosis and reverse osmosis processes for seawater desalination, Desalination 336 (1) (2014) 50–57.

[20] K. Lutchmiah, A.R.D. Verliefde, K. Roest, L.C. Rietveld, E.R. Cornelissen, Forward osmosis for application in wastewater treatment: a review, Water Res. 58 (2014) 179–197.

[21] Y. Feng, G. Han, L. Zhang, S.B. Chen, T.S. Chung, M. Weber, C. Maletzko, Rheology and phase inversion behavior of polyphenylenesulfone (PPSU) and sulfonated PPSU for membrane formation, Polymer 99 (2016) 72–82.

[22] K.Y. Wang, T.S. Chung, J.J. Qin, Polybenzimidazole (PBI) nanofiltration hollow fiber membranes applied in forward osmosis process, J. Membr. Sci. 300 (2007) 6–12.

[23] A.A. Alobaidy, B.Y. Sherhan, A.D. Barood, Q.F. Alsalhy, Effect of bore fluid flow rate on formation and properties of hollow fibers, Appl. Water Sci. 7 (8) (2017) 4387–4398.

[24] Q.F. Alsalhy, K.T. Rashid, S.S. Ibrahim, A.H. Ghanim, B. Van der Bruggen, P. Luis, M. Zablouk, Poly (vinylidene fluoride-co-hexafluoropropylene)(PVDF-co-HFP) hollow fiber membranes prepared from PVDF-co-HFP/PEG-600Mw/DMAC solution for membrane distillation, J. Appl. Polym. Sci. 129 (6) (2013) 3304–3313.

[25] Q.F. Alsalhy, K.T. Rashid, W.A. Noori, A. Figoli, S. Simone, E. Drioli, Poly (vinyl chloride) hollow fibers membranes for ultrafiltration applications: effects of internal coagulant composition, J. Appl. Polym. Sci. 124 (2012) 2087–2099.

[26] M. Shibuya, M. Yasukawa, S. Mishima, Y. Tanaka, T. Takahashi, H. Matsuyama, A thin-film composite-hollow fiber forward osmosis membrane with a polyketone hollow fiber membrane as a support, Desalination 402 (2017) 33–41.

[27] J. Wei, C. Qui, C.Y. Tang, R. Wang, A.G. Fan, Synthesis and characterization of flat-sheet thin film composite forward osmosis membranes, J. Membr. Sci. 372 (1-2) (2011) 292–302.

[28] J. Su, Q. Yang, J.F. Teo, T.S. Chung, Cellulose acetate nanofiltration hollow fiber membranes for forward osmosis processes, J. Membr. Sci. 355 (1-2) (2010) 36–44.

[29] S. Loeb, L. Titelman, E. Korngold, J. Freiman, Effect of porous support fabric on osmosis through a Loeb-Sourirajan type asymmetric membrane, J. Membr. Sci. 129 (2) (1997) 243–249.

[30] V.M.M. Lobo, Mutual diffusion coefficients in aqueous electrolyte solutions (technical report), Pure Appl. Chem. 65 (12) (1993) 2613–2640.

[31] Q.F. Alsalhy, H.A. Salih, R.H. Melkon, Y.M. Mahdi, N.A. Abdul Karim, Effect of the preparation conditions on the morphology and performance of poly (imide) hollow fiber membranes, J. Appl. Polym. Sci. 131 (12) (2014).

[32] M. García-Payo, M. Essalhi, M. Khayet, Effects of PVDF-HFP concentration on membrane distillation performance and structural morphology of hollow fiber membranes, J. Membr. Sci. 347 (1-2) (2010) 209–219.

[33] Q.F. Alsalhy, Algebory Sufyan, G.M. Alwan, A. Figoli, S. Simone, E. Drioli, Hollow fiber ultrafiltration membranes from poly(vinyl chloride): preparation, morphologies and properties, Sep. Sci. Technol. 46 (14) (2011) 2199–2210.

[34] S. Darvishmanesh, F. Tasselli, J.C. Jansen, E. Tocci, F. Bazzarelli, P. Bernardo, B. Van der Bruggen, Preparation of solvent stable polyphenylsulfone hollow fiber nanofiltration membranes, J. Membr. Sci. 384 (1-2) (2011) 89–96.

[35] J.R. McCutcheon, R.L. McGinnis, M. Elimelech, A novel ammonia—carbon dioxide forward (direct) osmosis desalination process, Desalination 174 (1) (2005) 1–11.

[36] A. Tiraferri, N.Y. Yip, W.A. Phillip, J.D. Schiffman, M. Elimelech, Relating performance of thin-film composite forward osmosis membranes to support layer formation and structure, J. Membr. Sci. 367 (1-2) (2011) 340–352.

[37] N.Y. Yip, A. Tiraferri, W.A. Phillip, J.D. Schiffman, M. Elimelech, High performance thin-film composite forward osmosis membrane, Environ. Sci. Technol. 44 (10) (2010) 3812–3818.

[38] P. Zhong, X. Fu, T.S. Chung, M. Weber, C. Maletzko, Development of thin-film composite forward osmosis hollow fiber membranes using direct sulfonated

polyphenylenesulfone (sPPSU) as membrane substrates, Environ. Sci. Technol. 47 (13) (2013) 7430–7436.
[39] F. Niu, M. Huang, T. Cai, L. Meng, Effect of membrane thickness on properties of FO membranes with nanofibrous substrate, in: 2nd International Symposium on Resource Exploration and Environmental Science, IOP Conf. Series: Earth and Environmental Science, 170, 2018, 052005.
[40] R.W. Holloway, R. Maltos, J. Vanneste, T.Y. Cath, Mixed draw solutions for improved forward osmosis performance, J. Membr. Sci. 491 (2015) 121–131.
[41] R.C. Ong, T.S. Chung, J.S. de Wit, B.J. Helmer, Novel cellulose ester substrates for high performance flat-sheet thin-film composite (TFC) forward osmosis (FO) membranes, J. Membr. Sci. 473 (2015) 63–71.
[42] N. Widjojo, T.S. Chung, M. Weber, C. Maletzko, V. Warzelhan, A sulfonated polyphenylenesulfone (sPPSU) as the supporting substrate in thin film composite (TFC) membranes with enhanced performance for forward osmosis (FO), Chem. Eng. J. 220 (2013) 15–23.
[43] T.Y. Cath, A.E. Childress, M. Elimelech, Forward osmosis: principles, applications, and recent developments, J. Membr. Sci. 281 (1-2) (2006) 70–87.
[44] D. Roy, M. Rahni, P. Pierre, V. Yargeau, Forward osmosis for the concentration and reuse of process saline wastewater, Chem. Eng. J. 287 (2016) 277–284.
[45] S. Al-aibi, H.B. Mahood, A.O. Sharif, E. Alpay, H. Simcoe-Read, Evaluation of draw solution effectiveness in a forward osmosis process, Desalin. Water Treat. 57 (29) (2016) 13425–13432.
[46] W.A. Phillip, J.S. Yong, M. Elimelech, Reverse draw solute permeation in forward osmosis: modeling and experiments, Environ. Sci. Technol. 44 (13) (2010) 5170–5176.
[47] Hau Thi Nguyen, Nguyen Cong Nguyen, Shiao-Shing Chen, Huu Hao Ngo, Wenshan Guo, Chi-Wang Li, A new class of draw solutions for minimizing reverse salt flux to improve forward osmosis desalination, Sci. Total Environ. 538 (2015) 129–136.
[48] N.Q. Trung, P.T.P. Thao, Novel draw solutes of iron complexes easier recovery in forward osmosis process, J. Water Reuse Desalin. 8 (2) (2018) 244–250.
[49] R. Wang, L. Shi, C.Y. Tang, S. Chou, C. Qiu, A.G. Fane, Characterization of novel forward osmosis hollow fiber membranes, J. Membr. Sci. 355 (1-2) (2010) 158–167.
[50] X. Zhang, L. Shen, W.Z. Lang, Y. Wang, Improved performance of thin-film composite membrane with PVDF/PFSA substrate for forward osmosis process, J. Membr. Sci. 535 (2017) 188–199.
[51] G. Li, J. Wang, D. Hou, Y. Bai, H. Liu, Fabrication and performance of PET mesh enhanced cellulose acetate membranes for forward osmosis, J. Environ. Sci. 45 (2016) 7–17.
[52] J. Su, Q. Yang, J.F. Teo, T.S. Chung, Cellulose acetate nanofiltration hollow fiber membranes for forward osmosis processes, J. Membr. Sci. 355 (1-2) (2010) 36–44.
[53] K.Y. Wang, Q. Yang, T.S. Chung, R. Rajagopalan, Enhanced forward osmosis from chemically modified polybenzimidazole (PBI) nanofiltration hollow fiber membranes with a thin wall, Chem. Eng. Sci. 64 (7) (2009) 1577–1584.
[54] L. Setiawan, R. Wang, K. Li, A.G. Fane, Fabrication of novel poly (amide–imide) forward osmosis hollow fiber membranes with a positively charged nanofiltration-like selective layer, J. Membr. Sci. 369 (1-2) (2011) 196–205.
[55] M. Yasukawa, S. Mishima, M. Shibuya, D. Saeki, T. Takahashi, T. Miyoshi, H. Matsuyama, Preparation of a forward osmosis membrane using a highly porous polyketone microfiltration membrane as a novel support, J. Membr. Sci. 487 (2015) 51–59.
[56] Z. Zhou, J.Y. Lee, T.S. Chung, Thin film composite forward-osmosis membranes with enhanced internal osmotic pressure for internal concentration polarization reduction, Chem. Eng. J. 249 (2014) 236–245.
[57] S. Chou, L. Shi, R. Wang, C.Y. Tang, C. Qiu, A.G. Fane, Characteristics and potential applications of a novel forward osmosis hollow fiber membrane, Desalination 261 (3) (2010) 365–372.
[58] S. Sahebi, S. Phuntsho, Y.C. Woo, M.J. Park, L.D. Tijing, S. Hong, H.K. Shon, Effect of sulphonated polyethersulfone substrate for thin film composite forward osmosis membrane, Desalination 389 (2016) 129–136.
[59] P. Nasr, H. Sewilam, Investigating the performance of ammonium sulphate draw solution in fertilizer drawn forward osmosis process, Clean Technol. Environ. Policy 18 (3) (2016) 717–727.
[60] M. Ghanbari, D. Emadzadeh, W.J. Lau, H. Riazi, D. Almasi, A.F. Ismail, Minimizing structural parameter of thin film composite forward osmosis membranes using polysulfone/halloysite nanotubes as membrane substrates, Desalination 377 (2016) 152–162.
[61] S. Zou, Z. He, Enhancing wastewater reuse by forward osmosis with self-diluted commercial fertilizers as draw solutes, Water Res. 99 (2016) 235–243.
[62] S. Shokrollahzadeh, S. Tajik, Fabrication of thin film composite forward osmosis membrane using electrospun polysulfone/polyacrylonitrile blend nanofibers as porous substrate, Desalination 425 (2018) 68–76.
[63] Katie C. Kedwell, Cejna A. Quist-Jensen, Georgios Giannakakis, Morten L. Christensen, Forward osmosis with high-performing TFC membranes for concentration of digester centrate prior to phosphorus recovery, Separation and Purification Technology, Sep. Purif. Technol. 197 (2018) 449–456.
[64] Lingling Xia, Mads Friis Andersen, Claus Hélix-Nielsen, Jeffrey R. McCutcheon, Novel commercial aquaporin flat-sheet membrane for forward osmosis, Ind. Eng. Chem. Res. 56 (41) (2017) 11919–11925.